On Multistreaming with Electrically Small Antenna Arrays

Michel T. Ivrlač and Josef A. Nossek
Institute for Circuit Theory and Signal Processing
Technische Universität München, D-80333 Munich, Germany
email: {ivrlac, nossek}@tum.de

***Abstract*—We report on our research about the multistreaming capability of electrically small antenna arrays. It is shown that the near-field interaction of the closely spaced antennas accounts for a surprisingly good multistreaming capability. This is demonstrated for a 2×2 system of thin half-wavelength dipoles in a multipath environment provided by two reflector plates, and isotropic background noise. Decoupling/power-matching and decoupling/noise-matching networks are applied at the transmit side and the receive side arrays, respectively. In the absence of heat loss in the matching networks and antennas, the simultaneous transfer of two data streams is supported even in the extreme case where the electrical separation of the antennas in the arrays approaches zero.**

I. Introduction

Communication systems which use more than one antenna at both the transmitting and the receiving end of the link (so-called multi-input multi-output (MIMO) systems), potentially support the transfer of several data streams at the same time using the same band of frequencies. In order for this so-called *multistreaming* to work, the propagation channel must allow the transmitted signal to travel to the receiver over a number of sufficiently different paths in space, and arrive there simultaneously from different directions. This spatial structure of the channel can then be exploited by spatial signal processing at the transmit and the receive side to establish a number of independent communication channels [1]. Usually this requires the antennas inside the array to be spaced sufficiently far apart such that they can obtain substantially different samples of the electromagnetic field. On the other hand, when the antenna separation is small, the field samples are similar and eventually become almost the same as the distance between neighboring antennas decreases further towards zero. As this happens, the wave propagation becomes the same between any pair of transmit and receive antennas, making the two arrays essentially look like single antennas. The arrays can no longer distinguish between different directions, which makes multistreaming with very compact antenna arrays impossible [2].

This standard argument from the signal processing literature ignores, however, the electromagnetic interaction of antennas with each other and the electromagnetic field. This interaction causes a number of interesting effects to occur which are important for the multistreaming capability. The electromagnetic field is *changed* by the presence of the electric currents flowing in the antenna [3]. Also, *coupling* occurs between the otherwise independent sources of *noise* inside the receiver front-ends [4]. Moreover, the noise received by the antenna array in an isotropic background noise environment is necessarily *correlated* when the antennas are placed close to each other [5]. Moreover, *impedance matching* networks which are connected between the antenna ports and the inputs of the low-noise amplifiers, or the outputs of the high power amplifiers impact the properties of the system. When all these effects are taken into account and made use of by proper engineering, it turns out that multistreaming may still work well even with compact antenna arrays. We demonstrate this by analyzing a 2×2-MIMO system of half-wavelength dipoles and matching networks in a simple multipath environment consisting of two metallic reflection plates. Circuit theoretic multiport analysis shows that in the absence of heat loss the multistreaming capability can be maintained even when the distance between neighboring antennas in the array approaches zero.

II. System under Consideration

Consider two antenna arrays shown on the left hand side of Figure 1, each composed of two thin and lossless half wavelength dipoles. One array is used for transmission the other for reception. The dipoles are oriented parallel to the z-axis. There are two ideal metallic reflection plates placed in the middle between the two arrays and oriented parallel to the y-z-plane. These reflectors ensure that there is multipath transmission and reception, which is necessary to successfully employ multistreaming. The circuit theoretic multiport model of this system is shown on the right hand side, which also includes the high power amplifiers (HPA), the low-noise amplifiers (LNA) and two lossless impedance matching networks. The HPAs are assumed to be linear and modeled as ideal voltage sources with a series resistance R. The open-circuit generator voltage vector $\boldsymbol{u}_\mathrm{G} \in \mathbb{C}^{2\times1} \cdot \mathrm{V}$ contains the information that we want to transfer to the receiver. The generators are connected to an impedance matching network which operation is described by:

$$\begin{bmatrix} \boldsymbol{u}_\mathrm{T} \\ \boldsymbol{u}_\mathrm{A} \end{bmatrix} = \boldsymbol{Z}_\mathrm{MT} \begin{bmatrix} \boldsymbol{i}_\mathrm{T} \\ -\boldsymbol{i}_\mathrm{A} \end{bmatrix}, \qquad (1)$$

where $\boldsymbol{Z}_\mathrm{MT} \in \mathbb{C}^{4\times4} \cdot \Omega$ is its impedance matrix, and the port voltage vectors $\boldsymbol{u}_\mathrm{T}$, $\boldsymbol{u}_\mathrm{A} \in \mathbb{C}^{2\times1} \cdot \mathrm{V}$, and the corresponding port current vectors $\boldsymbol{i}_\mathrm{T}, \boldsymbol{i}_\mathrm{A} \in \mathbb{C}^{2\times1} \cdot \mathrm{A}$ are defined in Figure 1. We assume that the transmit impedance matching network is *reciprocal* and *lossless*, which necessitates that $\boldsymbol{Z}_\mathrm{MT}$ is a *symmetric matrix with vanishing real-part* [6]. Modeling the coupling between all pairs of the four antennas is taken care of by the antenna multiport, described by:

$$\begin{bmatrix} \boldsymbol{u}_\mathrm{A} \\ \boldsymbol{u}_\mathrm{B} \end{bmatrix} = \boldsymbol{Z}_\mathrm{A} \begin{bmatrix} \boldsymbol{i}_\mathrm{A} \\ \boldsymbol{i}_\mathrm{B} \end{bmatrix} = \begin{bmatrix} \boldsymbol{Z}_\mathrm{AT} & \boldsymbol{Z}_\mathrm{ATR} \\ \boldsymbol{Z}_\mathrm{ART} & \boldsymbol{Z}_\mathrm{AR} \end{bmatrix} \begin{bmatrix} \boldsymbol{i}_\mathrm{A} \\ \boldsymbol{i}_\mathrm{B} \end{bmatrix}, \qquad (2)$$

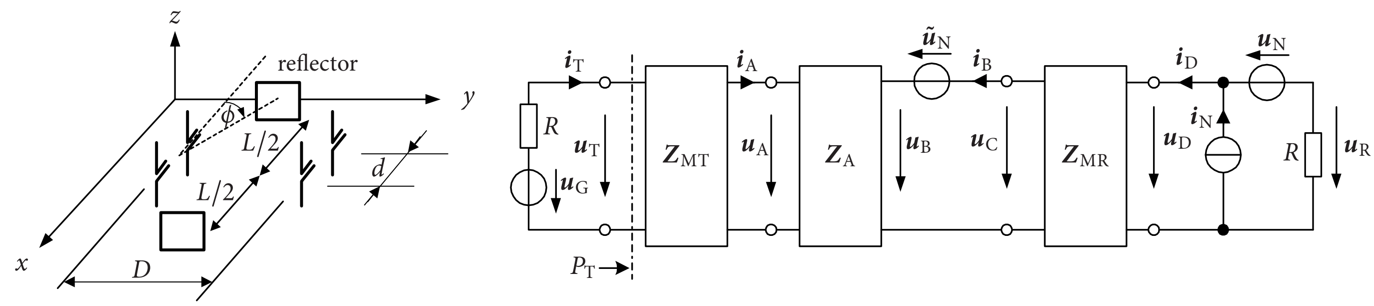

Figure 1: Left: Geometrical setup of the multiantenna system under consideration. Right: Multiport system model comprising (from left to right) high-power amplifiers, transmit impedance matching network, noisy antenna multiport, receive impedance matching network, and low-noise amplifiers.

where $\boldsymbol{Z}_\mathrm{A} \in \mathbb{C}^{4\times4}\cdot\Omega$ is its impedance matrix which is composed of the *transmit impedance matrix* $\boldsymbol{Z}_\mathrm{AT} \in \mathbb{C}^{2\times2}\cdot\Omega$, that describes the mutual coupling between the transmit side antennas, the *receive impedance matrix* $\boldsymbol{Z}_\mathrm{AR} \in \mathbb{C}^{2\times2}\cdot\Omega$, which describes the mutual coupling between the receive side antennas, and finally, the *transimpedance matrix* $\boldsymbol{Z}_\mathrm{ART} \in \mathbb{C}^{2\times2}\cdot\Omega$, that describes the mutual coupling between each pair of transmit and receive side antennas. Because antennas are reciprocal there is $\boldsymbol{Z}_\mathrm{A} = \boldsymbol{Z}_\mathrm{A}^\mathrm{T}$, which says that $\boldsymbol{Z}_\mathrm{ATR} = \boldsymbol{Z}_\mathrm{ART}^\mathrm{T}$, and that both $\boldsymbol{Z}_\mathrm{AT}$ and $\boldsymbol{Z}_\mathrm{AR}$ are symmetric matrices. The impedance matrix $\boldsymbol{Z}_\mathrm{A}$ only describes a noiseless antenna array. In reality, even lossless antennas are noisy due to the reception of background noise. When this background noise impinges *isotropically*, it can be shown that the *open-circuit* antenna noise voltage vector $\tilde{\boldsymbol{u}}_\mathrm{N} \in \mathbb{C}^{2\times1}\cdot\mathrm{V}$, has the correlation matrix [5]:

$$\mathrm{E}\left[\tilde{\boldsymbol{u}}_\mathrm{N}\tilde{\boldsymbol{u}}_\mathrm{N}^\mathrm{H}\right] = 4\mathrm{k}T_\mathrm{A}\Delta f\,\mathrm{Re}\{\boldsymbol{Z}_\mathrm{AR}\}, \tag{3}$$

where k is Boltzmann's constant, T_A is the *noise temperature* of the antenna, and Δf is the bandwidth. The noisy antenna ports are connected to one side of another impedance matching network, described by:

$$\begin{bmatrix}\boldsymbol{u}_\mathrm{D}\\ \boldsymbol{u}_\mathrm{C}\end{bmatrix} = \boldsymbol{Z}_\mathrm{MR}\begin{bmatrix}\boldsymbol{i}_\mathrm{D}\\ -\boldsymbol{i}_\mathrm{B}\end{bmatrix}, \tag{4}$$

where $\boldsymbol{Z}_\mathrm{MR} \in \mathbb{C}^{4\times4}\cdot\Omega$ is its impedance matrix, and the port voltage vectors $\boldsymbol{u}_\mathrm{C}, \boldsymbol{u}_\mathrm{D} \in \mathbb{C}^{2\times1}\cdot\mathrm{V}$, and the corresponding port current vectors $\boldsymbol{i}_\mathrm{B}, \boldsymbol{i}_\mathrm{D} \in \mathbb{C}^{2\times1}\cdot\mathrm{A}$ are defined in Figure 1. We assume that the receive impedance matching network is *reciprocal* and *lossless*, which necessitates that $\boldsymbol{Z}_\mathrm{MR}$ is a *symmetric matrix with vanishing real-part* [6]. The noise contributions of the LNAs can be modeled by inclusion of both a voltage noise $\boldsymbol{u}_\mathrm{N} \in \mathbb{C}^{2\times1}\cdot\mathrm{V}$, and a current noise $\boldsymbol{i}_\mathrm{N} \in \mathbb{C}^{2\times1}\cdot\mathrm{A}$, [7]. This is shown in the right-most part of Figure 1. We assume that the noise contributions of the two LNAs are uncorrelated, which is reasonable when the LNAs are independent devices. However, the noise voltage and the noise current corresponding to each LNA are usually correlated. Hence,

$$\mathrm{E}\left[\boldsymbol{i}_\mathrm{N}\boldsymbol{i}_\mathrm{N}^\mathrm{H}\right] = \beta\mathbf{I}_2,\;\; \mathrm{E}\left[\boldsymbol{u}_\mathrm{N}\boldsymbol{u}_\mathrm{N}^\mathrm{H}\right] = \beta R_\mathrm{N}^2\mathbf{I}_2,\;\; \mathrm{E}\left[\boldsymbol{u}_\mathrm{N}\boldsymbol{i}_\mathrm{N}^\mathrm{H}\right] = \rho\beta R_\mathrm{N}\mathbf{I}_2. \tag{5}$$

Here $\beta \in \mathbb{R}_+\cdot\mathrm{A}^2$ denotes the second moment of the noise current within a bandwidth Δf, and $R_\mathrm{N} = \sqrt{\mathrm{E}[|u_{\mathrm{N},j}|^2]/\mathrm{E}[|i_{\mathrm{N},j}|^2]}$, is the noise-resistance of the LNAs, while the complex noise correlation $\rho = \mathrm{E}[u_{\mathrm{N},j}\,i_{\mathrm{N},j}^*]/\sqrt{\mathrm{E}[|u_{\mathrm{N},j}|^2]\cdot\mathrm{E}[|i_{\mathrm{N},j}|^2]}$.

While it is true in general that in the equation (2), we have $\boldsymbol{Z}_\mathrm{ATR} = \boldsymbol{Z}_\mathrm{ART}^\mathrm{T}$, it is also true that in radio communications the signal attenuation between the transmitter and the receiver is usually extremely large. Hence, $\|\boldsymbol{Z}_\mathrm{ATR}\|_\mathrm{F} = \|\boldsymbol{Z}_\mathrm{ART}\|_\mathrm{F} \ll \|\boldsymbol{Z}_\mathrm{AT}\|_\mathrm{F}$ holds true in practice. This motivates to keep $\boldsymbol{Z}_\mathrm{ART}$ as it is, but to set $\boldsymbol{Z}_\mathrm{ATR} = \mathbf{O}_2$ in (2). This will be called the *unilateral approximation*. Because then $\boldsymbol{u}_\mathrm{A} \approx \boldsymbol{Z}_\mathrm{AT}\boldsymbol{i}_\mathbf{A}$, the electrical properties at the transmit side antenna ports are (almost) independent of what happens at the receiver.

III. Decoupling the Antenna Ports

In the noiseless case, the cascade of the antenna multiport and both impedance matching networks can be described (within the realm of the unilateral approximation) as:

$$\left.\begin{bmatrix}\boldsymbol{u}_\mathrm{T}\\ \boldsymbol{u}_\mathrm{D}\end{bmatrix}\right|_{\tilde{\boldsymbol{u}}_\mathrm{N}=\mathbf{0}} = \begin{bmatrix}\boldsymbol{Z}_\mathrm{T} & \mathbf{O}_2\\ \boldsymbol{Z}_\mathrm{RT} & \boldsymbol{Z}_\mathrm{R}\end{bmatrix}\begin{bmatrix}\boldsymbol{i}_\mathrm{T}\\ \boldsymbol{i}_\mathrm{D}\end{bmatrix}. \tag{6}$$

The transmit impedance matching network can be designed such that in (6): $\boldsymbol{Z}_\mathrm{T} = R\,\mathbf{I}_2$ holds true. In this way, the *antenna ports at the transmitter are decoupled* and each behaves like a resistance matching the internal impedance of the generators. Analyzing the circuit from Figure 1 shows that

$$\boldsymbol{Z}_\mathrm{MT} = \begin{bmatrix}\mathbf{O}_2 & -\mathrm{j}\sqrt{R}\,\mathrm{Re}\{\boldsymbol{Z}_\mathrm{AT}\}^{1/2}\\ -\mathrm{j}\sqrt{R}\,\mathrm{Re}\{\boldsymbol{Z}_\mathrm{AT}\}^{1/2} & -\mathrm{j}\,\mathrm{Im}\{\boldsymbol{Z}_\mathrm{AT}\}\end{bmatrix}, \tag{7}$$

ensures that $\boldsymbol{Z}_\mathrm{T} = R\,\mathbf{I}_2$ holds true. Note that $\boldsymbol{Z}_\mathrm{MT}$ from (7) is a symmetric matrix with vanishing real-part, thus it describes a reciprocal and lossless multiport. In a similar fashion, one can design the receive impedance matching network such that it has an impedance matrix given by:

$$\boldsymbol{Z}_\mathrm{MR} = \begin{bmatrix}\mathrm{j}\,\mathrm{Im}\{Z_\mathrm{opt}\}\,\mathbf{I}_2 & \mathrm{j}\sqrt{\mathrm{Re}\{Z_\mathrm{opt}\}}\,\mathrm{Re}\{\boldsymbol{Z}_\mathrm{AR}\}^{1/2}\\ \mathrm{j}\sqrt{\mathrm{Re}\{Z_\mathrm{opt}\}}\,\mathrm{Re}\{\boldsymbol{Z}_\mathrm{AR}\}^{1/2} & -\mathrm{j}\,\mathrm{Im}\{\boldsymbol{Z}_\mathrm{AR}\}\end{bmatrix}, \tag{8}$$

which leads in (6) to $\boldsymbol{Z}_\mathrm{R} = Z_\mathrm{opt}\mathbf{I}_2$. As a consequence, the *ports of the receiver's antennas become decoupled* and each provides a source with impedance $Z_\mathrm{opt} = R_\mathrm{N}\left(\sqrt{1-(\mathrm{Im}\{\rho\})^2} + \mathrm{j}\,\mathrm{Im}\{\rho\}\right)$, ensuring the receiver's noise figure is minimized [4]. Such antenna arrays with a decoupling network are realizations of multimode antennas [8].

IV. MIMO Channel Matrix

The impedance matching networks impact the effective transimpedance Z_{RT} in (6). The specific choice of the transmit and receive impedance matching networks according to (7) and (8) leads to:

$$\boldsymbol{Z}_{\mathrm{RT}} = \sqrt{R \cdot \mathrm{Re}\{Z_{\mathrm{opt}}\}}\, \mathrm{Re}\{\boldsymbol{Z}_{\mathrm{AR}}\}^{-1/2} \boldsymbol{Z}_{\mathrm{ART}}\, \mathrm{Re}\{\boldsymbol{Z}_{\mathrm{AT}}\}^{-1/2}. \quad (9)$$

While the impedance matching networks have done their job to decoupled the receiver's ports and the transmitter's ports, the mutual coupling *within* both arrays (in terms of $\mathrm{Re}\{\boldsymbol{Z}_{\mathrm{AR}}\}$ and $\mathrm{Re}\{\boldsymbol{Z}_{\mathrm{AT}}\}$), has reappeared by modifying the coupling *between* the transmitter and the receiver. Circuit analysis of the multiport in Figure 1, given the impedance matching networks from (7) and (8), reveals that the noise contaminated observable $\boldsymbol{u}_{\mathrm{R}} \in \mathbb{C}^{2\times 1} \cdot \mathrm{V}$ is given by:

$$\boldsymbol{u}_{\mathrm{R}} = \frac{1/2}{R + Z_{\mathrm{out}}} \boldsymbol{Z}_{\mathrm{RT}} \boldsymbol{u}_{\mathrm{G}} + \boldsymbol{n}, \quad (10)$$

where $\boldsymbol{n} \in \mathbb{C}^{2\times 1} \cdot \mathrm{V}$ is the resulting noise voltage with

$$\mathrm{E}\left[\boldsymbol{n}\boldsymbol{n}^{\mathrm{H}}\right] = \sigma_n^2 \mathbf{I}_2, \quad (11)$$

with

$$\sigma_n^2 = \frac{R^2 R_{\mathrm{N}}}{|R + Z_{\mathrm{opt}}|^2} \sqrt{1 - (\mathrm{Im}\{\rho\})^2}\, 4\mathrm{k} T_{\mathrm{A}} \Delta f\, \mathrm{NF}_{\mathrm{min}}. \quad (12)$$

Herein, $\mathrm{NF}_{\mathrm{min}}$ is the minimum noise figure [4]:

$$\mathrm{NF}_{\mathrm{min}} = 1 + \frac{\beta R_{\mathrm{N}}}{2\mathrm{k} T_{\mathrm{A}} \Delta f} \cdot \left(\sqrt{1 - (\mathrm{Im}\{\rho\})^2} - \mathrm{Re}\{\rho\}\right). \quad (13)$$

It is reasonable to define *transmit power* P_{T} as the total electric power which is delivered by the generators into the transmit impedance matching network, as indicated on the left hand side of Figure 1. Thus, $P_{\mathrm{T}} = \mathrm{E}[\mathrm{Re}\{\boldsymbol{u}_{\mathrm{T}}^{\mathrm{H}} \boldsymbol{i}_{\mathrm{T}}\}]$. From (6), we have $\boldsymbol{u}_{\mathrm{T}} = \boldsymbol{Z}_{\mathrm{T}} \boldsymbol{i}_{\mathrm{T}}$, and the transmit impedance matching network ensures that $\boldsymbol{Z}_{\mathrm{T}} = R\mathbf{I}_2$. The latter implies that $\boldsymbol{u}_{\mathrm{T}} = \tfrac{1}{2}\boldsymbol{u}_{\mathrm{G}}$, thus:

$$P_{\mathrm{T}} = \tfrac{1}{4}\mathrm{E}\left[\|\boldsymbol{u}_{\mathrm{G}}\|_2^2\right]/R. \quad (14)$$

It is convenient to define a *channel input vector* $\boldsymbol{x}$ as a scaled version of the generator voltage vector $\boldsymbol{u}_{\mathrm{G}}$, and a *channel output vector* $\boldsymbol{y}$ as a scaled version of the noisy observation $\boldsymbol{u}_{\mathrm{R}}$:

$$\boldsymbol{x} = \frac{1}{2\sqrt{R}} \boldsymbol{u}_{\mathrm{G}}, \quad \boldsymbol{y} = \frac{|R + Z_{\mathrm{opt}}|}{R\sqrt{R_{\mathrm{N}}\sqrt{1 - (\mathrm{Im}\{\rho\})^2}}} \boldsymbol{u}_{\mathrm{R}}. \quad (15)$$

Applying (15) to (10), it follows with the help of (9) and (12):

$$\boldsymbol{y} = \tilde{\boldsymbol{H}}\boldsymbol{x} + \boldsymbol{\vartheta}, \quad (16)$$

where $\boldsymbol{\vartheta}$ contains noise samples with correlation matrix:

$$\mathrm{E}\left[\boldsymbol{\vartheta}\boldsymbol{\vartheta}^{\mathrm{H}}\right] = \sigma_\vartheta^2 \mathbf{I}_2, \quad \sigma_\vartheta^2 = 4\mathrm{k} T_{\mathrm{A}} \Delta f\, \mathrm{NF}_{\mathrm{min}}, \quad (17)$$

hence, samples of *white* noise. Moreover,

$$P_{\mathrm{T}} = \mathrm{E}\left[\|\boldsymbol{x}\|_2^2\right], \quad (18)$$

and is, thus, the mean squared Euclidean norm of the channel input vector $\boldsymbol{x}$. In this way, (16) is a standard MIMO system model, with the MIMO channel matrix $\tilde{\boldsymbol{H}} \in \mathbb{C}^{2\times 2}$ given by:

$$\tilde{\boldsymbol{H}} = \mathrm{e}^{-\mathrm{j}\varphi}\, \mathrm{Re}\{\boldsymbol{Z}_{\mathrm{AR}}\}^{-1/2} \boldsymbol{Z}_{\mathrm{ART}}\, \mathrm{Re}\{\boldsymbol{Z}_{\mathrm{AT}}\}^{-1/2}, \quad (19)$$

where $\varphi = \mathrm{angle}\left(R + Z_{\mathrm{opt}}\right)$. Clearly, the unimodular constant term $\mathrm{e}^{-\mathrm{j}\varphi}$ has no impact on performance, so that it can safely be neglected in information theory, replacing $\tilde{\boldsymbol{H}}$ by:

$$\boldsymbol{H} = \mathrm{Re}\{\boldsymbol{Z}_{\mathrm{AR}}\}^{-1/2} \boldsymbol{Z}_{\mathrm{ART}}\, \mathrm{Re}\{\boldsymbol{Z}_{\mathrm{AT}}\}^{-1/2}. \quad (20)$$

A beautiful aspect of this result is that, from an information theory perspective, there is *no* need to know any of the internal details, such as R, R_{N}, ρ, and Z_{opt}. All that matters is condensed into the channel matrix given in (20), and can be obtained *solely* and readily from parts of the array impedance matrix $\boldsymbol{Z}_{\mathrm{A}}$.

V. The Array Impedance Matrix

Computing the array impedance matrix, let us first consider a single half-wavelength dipole in the origin O of a Cartesian coordinate system and lined up with its z-axis. With a current i flowing through the dipole's excitation port, the resulting electric field at a point P in the *far-field* is given in spherical coordinates as (e.g., [9], page 153):

$$\vec{E} = \vec{\mathbf{e}}_\theta \frac{\mathrm{j} i \mathrm{e}^{-\mathrm{j}2\pi r/\lambda}}{2\pi r \epsilon_0 c} \cdot \frac{\cos\left(\tfrac{1}{2}\pi \cos\theta\right)}{\sin\theta}, \quad (21)$$

where λ is the wave length, r the distance of the point P to the origin O, and θ the angle that $\overline{\mathrm{OP}}$ makes with the z-axis. Moreover, ϵ_0 is the electric constant, and c is the speed of light. Now let the point P be in the x-y-plane, such that $\theta = \pi/2$. If another $\lambda/2$-dipole is located in P and oriented in parallel to the first dipole (i.e., in the direction of the z-axis), then the open-circuit voltage that is induced into this dipole is given by the product of the electric field strength and the dipole's effective length l_{eff} (e.g., [9], page 80). Because $l_{\mathrm{eff}} = \lambda/\pi$ for a $\lambda/2$ dipole (e.g., [3], page 509), the transimpedance of these two dipoles equals:

$$Z_{\mathrm{ART}} = \frac{\mathrm{e}^{-\mathrm{j}2\pi r/\lambda}}{r} \cdot \frac{\mathrm{j}\lambda}{2\pi^2 \epsilon_0 c}, \quad r \gg \lambda. \quad (22)$$

Consider now the scenario from the left hand side of Figure 1. The transmitter's and the receiver's array are separated by the distance D, while the two $\lambda/2$-dipoles inside each array are spaced a distance d apart. Two symmetrically located metallic reflection plates provide a defined multi-path environment. They are set a distance L apart. When a line were drawn from the center of each array to the center of each reflection plate, it would make an angle ϕ with the array line-ups (parallel to the x-axis). The distance D is assumed to be large enough such that the partner array and the reflectors are well in the far field. We assume in the following that the wave propagation can be approximated accurately enough by quasi optical rays with perfect reflections. Because there are three paths (a direct path and two paths over the reflection plates) by which the transmitter can reach the receiver, the transimpedance matrix $\boldsymbol{Z}_{\mathrm{ART}}$ can be written as the sum of three components:

$$\boldsymbol{Z}_{\mathrm{ART}} = \boldsymbol{Z}_{\mathrm{ART},1} + \boldsymbol{Z}_{\mathrm{ART},2} + \boldsymbol{Z}_{\mathrm{ART},3}, \quad (23)$$

where (applying (22) for each pair of distant antennas)

$$\boldsymbol{Z}_{\mathrm{ART},1} = \frac{\alpha \mathrm{e}^{-\mathrm{j}2\pi D/\lambda}}{D} \begin{bmatrix} 1 & 1 \\ 1 & 1 \end{bmatrix}, \quad \text{with } \alpha = \frac{\mathrm{j}\lambda}{2\pi^2 \epsilon_0 c}, \quad (24)$$

corresponds to the direct path, and

$$\boldsymbol{Z}_{\mathrm{ART},2,3} = \frac{-\alpha \mathrm{e}^{-\mathrm{j}2\pi r/\lambda}}{r} \begin{bmatrix} \mathrm{e}^{\pm \mathrm{j}2\pi \frac{d}{\lambda}\cos\phi} & 1 \\ 1 & \mathrm{e}^{\mp \mathrm{j}2\pi \frac{d}{\lambda}\cos\phi} \end{bmatrix} \quad (25)$$

correspond to the paths over the two reflection plates, respectively. Herein, r is the distance from the center of the transmitter's array to the center of the receiver's array, taking the longer way over the reflection plates:

$$r = D/\sin\phi. \quad (26)$$

The negative sign of the factor α in (25) is due to the reflected waves having to change their phase by 180 degrees, because the incident field is polarized *tangential* to the reflectors. Using the relationship $D/r = \sin\phi$ from (26), we can rewrite (23) as:

$$\boldsymbol{Z}_{\mathrm{ART}} = \frac{\alpha \mathrm{e}^{-\mathrm{j}2\pi D/\lambda}}{D} \begin{bmatrix} \tilde{a} & \tilde{b} \\ \tilde{b} & \tilde{a} \end{bmatrix}, \quad \begin{aligned} \tilde{a} &= 1 - 2\mathrm{e}^{-\mathrm{j}\Psi}\sin(\phi)\cos(2\pi\tfrac{d}{\lambda}\cos\phi) \\ \tilde{b} &= 1 - 2\mathrm{e}^{-\mathrm{j}\Psi}\sin\phi, \end{aligned} \quad (27)$$

where we have introduced the variable

$$\Psi = \frac{2\pi D}{\lambda}\left(\frac{1}{\sin\phi} - 1\right), \quad (28)$$

for notational convenience. Now what happens when the distance d of the dipoles inside the arrays is made smaller and smaller? It is clear from (27) that $\boldsymbol{Z}_{\mathrm{ART}}$ will tend to become a rank one matrix:

$$\lim_{d/\lambda\to 0} \boldsymbol{Z}_{\mathrm{ART}} = \frac{\alpha \mathrm{e}^{-\mathrm{j}kD}}{D}\left(1 - 2\mathrm{e}^{-\mathrm{j}\Psi}\sin\phi\right)\begin{bmatrix} 1 & 1 \\ 1 & 1 \end{bmatrix}. \quad (29)$$

Because of this it is usually argued that by making d smaller and smaller, the two antennas in each array essentially look like a single antenna, making multi-streaming more and more difficult, and ultimately impossible as $d/\lambda \to 0$. However, recall that from an information theory point of view, it is *not* $\boldsymbol{Z}_{\mathrm{ART}}$ which is the relevant MIMO channel matrix, but rather the matrix $\boldsymbol{H}$ given in (20). Therefore, in order to find $\boldsymbol{H}$, we also have to find the real-parts of the transmit and receive array impedance matrices, which account for the mutual coupling of the antennas *within* the arrays (*intra-array* coupling), in addition to $\boldsymbol{Z}_{\mathrm{ART}}$, which describes the mutual coupling *between* the arrays (*inter-array* coupling). Now it is an interesting fact that the real-part of the normalized array impedance matrix (normalized such that the main diagonal is unity) for two colinear $\lambda/2$-dipoles is almost exactly the same as the normalized array impedance matrix of two Hertzian dipoles [10]. One therefore obtains: [10], [11]:

$$\mathrm{Re}\{\boldsymbol{Z}_{\mathrm{AT}}\} = \mathrm{Re}\{\boldsymbol{Z}_{\mathrm{AR}}\} = 73\Omega \begin{bmatrix} 1 & \Theta(2\pi d/\lambda) \\ \Theta(2\pi d/\lambda) & 1 \end{bmatrix}, \quad (30)$$

where

$$\Theta(x) = \frac{3}{2}\left(\frac{\sin x}{x} + \frac{\cos x}{x^2} - \frac{\sin x}{x^3}\right). \quad (31)$$

Notice that as $d/\lambda \to 0$, the rank of these impedance matrices becomes unity. Because in (20), these matrices appear with their *inverse* square root, it is possible that the channel matrix $\boldsymbol{H}$ *retains full rank,* despite that $\boldsymbol{Z}_{\mathrm{ART}}$, $\mathrm{Re}\{\boldsymbol{Z}_{\mathrm{AT}}\}$, and $\mathrm{Re}\{\boldsymbol{Z}_{\mathrm{AR}}\}$ all tend to rank-deficient matrices. Let us look now into this.

VI. Super-Compact MIMO System

By substituting (31) into (30) and the latter together with (27) into (20), one can calculate the actual MIMO channel matrix $\boldsymbol{H}$. To this end, one can make use of the fact that:

$$\begin{bmatrix} 1 & \Theta \\ \Theta & 1 \end{bmatrix}^{-1/2} \begin{bmatrix} \tilde{a} & \tilde{b} \\ \tilde{b} & \tilde{a} \end{bmatrix} \begin{bmatrix} 1 & \Theta \\ \Theta & 1 \end{bmatrix}^{-1/2} = \frac{1}{1-\Theta^2}\begin{bmatrix} \tilde{a} - \tilde{b}\Theta & \tilde{b} - \tilde{a}\Theta \\ \tilde{b} - \tilde{a}\Theta & \tilde{a} - \tilde{b}\Theta \end{bmatrix}. \quad (32)$$

Asymptotically, letting the electric distance $d/\lambda \to 0$, one obtains a *super-compact* MIMO system with channel matrix:

$$\boldsymbol{H}_0 = \lim_{d/\lambda\to 0} \boldsymbol{H} = \gamma \begin{bmatrix} a & b \\ b & a \end{bmatrix}, \quad \begin{aligned} a &= 4\mathrm{e}^{\mathrm{j}\Psi} - 3\sin(\phi) + 5\sin 3\phi \\ b &= 4\mathrm{e}^{\mathrm{j}\Psi} - 13\sin(\phi) - 5\sin 3\phi, \end{aligned} \quad (33)$$

where

$$\gamma = \frac{\mathrm{j}1.64\mathrm{e}^{-\mathrm{j}2\pi D/\lambda}}{2\pi D/\lambda} \cdot \frac{\mathrm{e}^{-\mathrm{j}\Psi}}{8}. \quad (34)$$

As $\det \boldsymbol{H}_0 = \gamma^2\, 80\left(\mathrm{e}^{\mathrm{j}\Psi} - 2\sin\phi\right)\left(\sin(\phi) + \sin 3\phi\right)$, we can see that, in general, $\boldsymbol{H}_0$ *has full rank which makes multi-streaming possible even for arbitrarily small antenna separation d/λ inside the arrays.*

In order to obtain more insight we should look at the eigenvalues of $\boldsymbol{H}_0^{\mathrm{H}}\boldsymbol{H}_0$, for they are directly related to the information theoretic channel capacity [1].

$$\boldsymbol{H}_0^{\mathrm{H}}\boldsymbol{H}_0 = \boldsymbol{V}\begin{bmatrix} \xi_1 & 0 \\ 0 & \xi_2 \end{bmatrix}\boldsymbol{V}^{\mathrm{H}}. \quad (35)$$

The eigenvalues ξ_1 and ξ_2 compute to:

$$\left.\begin{aligned} \xi_1 &= |\gamma|^2\, 64\left(3 - 2\cos(2\phi) - 4\cos(\Psi)\sin\phi\right), \\ \xi_2 &= |\gamma|^2\, 1600\cos^4(\phi)\sin^2\phi. \end{aligned}\right\} \quad (36)$$

Of course, it is good to have as large eigenvalues as possible, so that from (36) we see that Ψ should be chosen such that $\cos\Psi = -1$, because $\sin\phi \geq 0$. Hence:

$$\Psi_{\mathrm{opt}} = \pi + n\cdot 2\pi, \quad n \in \{0, \pm1, \pm2, \cdots\}. \quad (37)$$

Substituting Ψ_{opt} for Ψ in (36), it turns out that $\xi_1 > \xi_2$. Hence, we obtain for the eigenvalue ratio:

$$\frac{\xi_{\min}}{\xi_{\max}} = \frac{\xi_2}{\xi_1} = 25\frac{\cos^4(\phi)\sin^2\phi}{(1+2\sin\phi)^2} < 1. \quad (38)$$

Effective multistreaming requires that both these eigenvalues are similar, for otherwise the system supports one »strong« and one »weak« data stream. The weak data stream, contributing only marginally to the total channel capacity, would make multistreaming much less effective. Because $\xi_{\min}/\xi_{\max} < 1$, it is clear that the ideal case of having identical eigenvalues does not happen for the super-compact MIMO system under consideration. However, one can bring the ratio $\xi_{\min}/\xi_{\max}$ as close to unity as possible by maximization with respect to the angle ϕ. Taking the first derivative of (38) with respect to ϕ and setting it to zero, we find that $\phi_{\mathrm{opt}} \approx 27°$. By letting $\Psi = \Psi_{\mathrm{opt}}$, and $\phi = \phi_{\mathrm{opt}}$, it follows with (28) and (37) that the optimum distance D_{opt} is given by

$$D_{\mathrm{opt}} = \lambda\frac{n + ½}{-1 + 1/\sin\phi_{\mathrm{opt}}}. \quad (39)$$

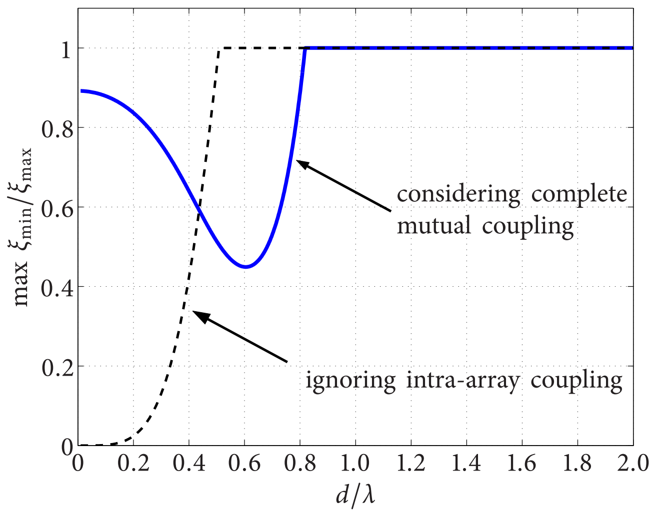

Figure 2: Smallest achievable eigenvalue spread of $\boldsymbol{H}^{\mathrm{H}}\boldsymbol{H}$.

Using the numerical value for $\phi_{\mathrm{opt}} \approx 27°$, we obtain

$$D_{\mathrm{opt}} \approx 0.836\lambda \cdot (n + ½), \quad n \in \mathbb{N}, \ n \gg 1. \tag{40}$$

Finally, we can also give the optimum distance L between the reflectors explicitly:

$$L_{\mathrm{opt}} = D_{\mathrm{opt}} / \tan \phi_{\mathrm{opt}} \approx 1.955 \cdot D_{\mathrm{opt}}. \tag{41}$$

When $\phi = \phi_{\mathrm{opt}}$, we obtain from (38) that

$$\max \frac{\xi_{\min}}{\xi_{\max}} \approx 0.892. \tag{42}$$

Now this ratio of eigenvalues of $\boldsymbol{H}_0^{\mathrm{H}}\boldsymbol{H}_0$ is pretty close to unity. In fact, $\xi_{\min}$ is less than 0.5dB below $\xi_{\max}$. This means that *effective multistreaming is possible even if the electrical antenna separation inside the arrays approaches zero.*

VII. Compact MIMO System

While the asymptotic analysis where we let $d/\lambda \to 0$ is interesting and insightful, a real MIMO system will always have finite d/λ. In the following, we therefore have a look at the system from Figure 1 with variable distance d. The solid curve in Figure 2 shows the quantity

$$\Psi = \max_{\phi} \frac{\xi_{\min}}{\xi_{\max}},$$

as a function of d/λ. One can spot a number of interesting observations. For a relatively large antenna separation, characterized by $d > 0.82\lambda$, there always is some way or other to place the reflection plates which result in a unity Ψ. This represents the best use of multistreaming because two streams can be supported with *perfectly equal* share of the total channel capacity. Now when we reduce d below 0.82λ, we see that Ψ begins to drop until it reaches its global minimum of $\Psi_{\min} \approx 0.45$ at an antenna separation of about 0.61λ. It is quite remarkable that a relatively large separation of $d = 0.61\lambda$ is the worst case with respect to multistream transmission, where even the best placing of the reflection plates will result in more than 3dB eigenvalue spread. However, as we decrease the distance d further, remarkably enough, Ψ begins to *increase* again, ultimately reaching the limit of 0.892, as $d \to 0$. In fact, compact arrays, with $d \leq 0.25\lambda$, can allow for remarkably effective multistream operation. The dashed curve in Figure 2 shows the hypothetical result for Ψ for the case where the intra-array coupling, i.e., mutual coupling between antennas inside the arrays, is ignored. This can be calculated by merely setting the real-parts of $\boldsymbol{Z}_{\mathrm{AT}}$ and $\boldsymbol{Z}_{\mathrm{AR}}$ equal to scaled identity matrices, irrespective of the antenna separation d. This ignorance of intra-array coupling is commonplace in contemporary signal processing and information theory literature [2]. Without considering intra-array coupling the results for Ψ are remarkably different. Once d is reduced below $\lambda/2$, the hypothetical value of Ψ drops monotonically towards zero as d is reduced. This is in striking contrast to the large value of Ψ which actually results from taking the full antenna mutual coupling into account. Moreover, ignoring intra-array coupling does not predict the actual low value of Ψ for the relatively large separation of $d = 0.61\lambda$, thereby predicting falsely that Ψ is unity for $d \geq \lambda/2$. This demonstrates how important it is to take the full mutual antenna coupling into account not only for compact antenna arrays, but also for arrays with an antenna separation in the neighborhood of $\lambda/2$.

VIII. Conclusion

From a circuit theoretic multiport analysis, capturing all relevant physics of mutual antenna coupling, we have shown for a 2×2-MIMO system, composed of four thin half-wavelength dipoles and two reflecting plates in otherwise empty space, that, in the absence of heat loss, effective multistreaming remains possible even for arbitrarily small antenna separation inside the arrays, provided means are taken to decouple the antenna ports at both arrays, for example by employing decoupling multiports.

References

[1] I. E. Telatar, “Capacity of Multi-Antenna Gaussian Channels,” *European Transactions on Telecommunications*, vol. 10(6), pp. 585–596, nov 1999.

[2] D. Tse and P. Viswanath, *Fundamentals of Wireless Communication*. Cambridge University Press, 2005.

[3] S. A. Schelkunoff and H. T. Friis, *Antennas. Theory and Practice*. New York, NY: Wiley, 1952.

[4] M. T. Ivrlač and J. A. Nossek, “Toward a Circuit Theory of Communication,” *IEEE Transactions on Circuits and Systems I: Regular Papers*, vol. 57(7), pp. 1663–1683, 2010.

[5] R. Q. Twiss, “Nyquist’s and Thevenin’s Theorems Generalized for Nonreciprocal Linear Networks,” *J. Appl. Phys.*, vol. 26, pp. 599–602, May 1955.

[6] V. Belevitch, *Classical Network Theory*. Holden Day, San Francisco, 1968.

[7] H. Hillbrand and P. Russer, “An Efficient Method for Computer Aided Noise Analysis of Linear Amplifier Networks,” *IEEE Transactions on Circuits and Systems*, vol. 23(4), pp. 235–238, jun 1976.

[8] D. Eßer and H. J. Chaloupka, “Design Approach for a Class of Compact Multiport Antennas,” in *Proc. IEEE 2005 Int. Symp. on Microwave, Antenna, Propagat. and EMC Technol. for Wireless Commun. (MAPE 2005)*, 2005, pp. 144–147.

[9] A. Balanis, *Antenna Theory*. Second Edition, John Wiley & Sons, 1997.

[10] M. T. Ivrlač, “Lecture Notes on Circuit Theory and Communications (unpublished),” *Technische Universität München*, May 2010.

[11] H. Yordanov, M. T. Ivrlač, P. Russer, and J. A. Nossek, “Arrays of Isotropic Radiators — A Field-theoretic Justification,” in *Proc. of the IEEE/ITG International Workshop on Smart Antennas, 2009*, Berlin, Germany, feb 2009.